NEURAL REGENERATION RESEARCH
March 2017, Volume 12, Issue 3
www.nrronline.org

RESEARCH ARTICLE

Anatomical distributional defects in mutant genes associated with dominant intermediate Charcot-Marie-Tooth disease type C in an adenovirus-mediated mouse model

SeoJin Lee[1, #], Sandesh Panthi[1, #], Hyun Woo Jo[1], Jaeyoung Cho[2], Min-Sik Kim[3], Na Young Jeong[4], In Ok Song[5], Junyang Jung[1, 2, 6, *], Youngbuhm Huh[1, 2, 6, *]

1 Department of Biomedical Science, Graduate School, Kyung Hee University, Dongdaemun-gu, Seoul, Korea
2 Department of Medicine, Graduate School, Kyung Hee University, Dongdaemun-gu, Seoul, Korea
3 Department of Applied Chemistry, College of Applied Science, Kyung Hee University, Yongin-si, Gyeonggi-do, Korea
4 Department of Anatomy and Cell Biology, College of Medicine, Dong-A University, Seo-gu, Busan, Korea
5 Department of Reproductive Endocrinology and Infertility, Department of Obstetrics and Gynecology, Cheil General Hospital, Dankook University College of Medicine, Jung-gu, Seoul, Korea
6 Department of Anatomy and Neurobiology, College of Medicine, Kyung Hee University, Dongdaemun-gu, Seoul, Korea

How to cite this article: *Lee S, Panthi S, Jo HW, Cho J, Kim MS, Jeong NY, Song IO, Jung J, Huh Y (2017) Anatomical distributional defects in mutant genes associated with dominant intermediate Charcot-Marie-Tooth disease type C in an adenovirus-mediated mouse model. Neural Regen Res 12(3):486-492.*

Funding: *This work was supported by the National Research Foundation (NRF) of Korea grant funded by Korean Government (MEST) (No. 2011-0030072).*

Abstract

Dominant intermediate Charcot-Marie-Tooth disease type C (DI-CMTC) is a dominantly inherited neuropathy that has been classified primarily based on motor conduction velocity tests but is now known to involve axonal and demyelination features. DI-CMTC is linked to tyrosyl-tRNA synthetase (YARS)-associated neuropathies, which are caused by E196K and G41R missense mutations and a single *de novo* deletion (153-156delVKQV). It is well-established that these YARS mutations induce neuronal dysfunction, morphological symptoms involving axonal degeneration, and impaired motor performance. The present study is the first to describe a novel mouse model of YARS-mutation-induced neuropathy involving a neuron-specific promoter with a deleted mitochondrial targeting sequence that inhibits the expression of YARS protein in the mitochondria. An adenovirus vector system and *in vivo* techniques were utilized to express YARS fusion proteins with a Flag-tag in the spinal cord, peripheral axons, and dorsal root ganglia. Following transfection of YARS-expressing viruses, the distributions of wild-type (WT) YARS and E196K mutant proteins were compared in all expressed regions; G41R was not expressed. The proportion of Flag/green fluorescent protein (GFP) double-positive signaling in the E196K mutant-type mice did not significantly differ from that of WT mice in dorsal root ganglion neurons. All adenovirus genes, and even the empty vector without the YARS gene, exhibited GFP-positive signaling in the ventral horn of the spinal cord because GFP in an adenovirus vector is driven by a cytomegalovirus promoter. The present study demonstrated that anatomical differences in tissue can lead to dissimilar expressions of YARS genes. Thus, use of this novel animal model will provide data regarding distributional defects between mutant and WT genes in neurons, the DI-CMTC phenotype, and potential treatment approaches for this disease.

Key Words: *nerve regeneration; tyrosyl-tRNA synthetase; YARS-associated neuropathy; YARS mutation; Charcot-Marie-Tooth Disease; adenoviral vector-mediated mouse models; neural regeneration*

***Correspondence to:**
Junyang Jung, M.D., Ph.D. or Youngbuhm Huh, M.D., Ph.D., jjung@khu.ac.kr or ybhuh@khu.ac.kr.

#These authors contributed equally to this study.

orcid:
0000-0003-3946-5406 (Junyang Jung)
0000-0002-7687-0374 (Youngbuhm Huh)

doi: *10.4103/1673-5374.202920*

Accepted: *2017-03-07*

Introduction

Charcot-Marie-Tooth Disease (CMT) is an incurable neurological disorder that has historically been classified as a subtype of muscular dystrophy (Krajewski et al., 2000). It is a common hereditary motor and sensory neuropathy that is now believed to be the result of demyelination and/or the axonal degeneration of peripheral neurons (Jordanova et al., 2006). CMT was initially identified as a syndrome by the unified work of three scientists (Charcot and Marie, 1886; Tooth, 1886), and it was subsequently confirmed to be a peripheral nervous system (PNS) disorder by Hoffman (1889). Prior to 1977, the conventional method of classifying CMT patients included motor conduction velocity tests, and the term 'dominant intermediate' was adopted as a designation for patients with a dominant inheritance of CMT and median motor conduction velocities between 25–45 m/s (Davis et al., 1978). Subsequently, CMT has been characterized on the basis of its axonal and demyelination features

(Kennerson et al., 2001).

Tyrosyl-tRNA synthetase (YARS) is associated with dominant intermediate CMT neuropathy type C (DI-CMTC; (Jordanova et al., 2006). This enzyme catalyzes the aminoacylation of tRNA in a two-step process with tyrosine via its cognate amino acid (Fersht et al., 1975) and is thought to be one of the first proteins discovered due to its vital role in linking amino acids with nucleotide triplets contained in tRNAs (Pruitt et al., 2009). In addition to its essential role in protein biosynthesis, YARS also exhibits cytokine activities in humans such that the N-terminal aspect fosters the catalytic site following its fragmentation (Kleeman et al., 1997). Jordanova et al. (2006) identified two heterozygous missense mutations (G41R and E196K) and one *de novo* deletion (153-156delVKQV) in YARS that exhibit a linkage to DI-CMTC. The E196K and G41R mutations are present in the N-terminal aspect of YARS that contains the catalytic and anticodon recognition sites. Biochemical analyses have revealed that these two mutations lead to decreases in the ability to run the first step of aminoacylation (Antonellis and Green, 2008).

Adenoviral vector-mediated mouse models have been successfully used to identify cellular distribution patterns in cell molecules, induce molecular changes in various mutants, and enable the manifestation of functional and morphological phenotypes. Previous studies from our research group investigated glycyl-tRNA synthetase (GARS)-associated neuropathy by developing an adenoviral-mediated mouse model that was useful for characterizing the pathogeneses of CMT type 2D (CMT2D) and distal spinal muscular atrophy type V (dSMA-V) (Seo et al., 2014a, b). Utilizing *in vitro* techniques, Jordanova et al (2006) found reductions in the homogenous distributions of both mutant genes in transfected cells without preferential sorting to neuronal tips. In contrast, the non-transfected cells in that study exhibited distributional differences in both differentiating and undifferentiating neuronal cells in growth cones, branch points, and the distal aspects of neurite projections.

Thus, to confirm the effects of the YARS mutants in a mouse model of DI-CMTC, three mutant-expressing adenoviruses (YARS wild type [WT], E196K, and G41R) were designed from artificial human YARS (hYARS) clones. The findings demonstrate that the YARS mutants may explain the DI-CMTC phenotype as well as the associated distributional defects and differences.

Materials and Methods

Animals

Thirty-six 6-week-old male C57BL/6 mice were housed in a humidity- and temperature-controlled environment with *ad libitum* access to water and food. All animal procedures and sacrifices were performed in accordance with the guidelines of the Korean Academy of Medical Science and the approval of the KHU Committee of Animal Research (approval number: KHUASP[SE]-16-043). Sincere efforts were made to reduce the number of animals used in the study groups as well as to mitigate the pain and suffering experienced by the animals.

Neuron-specific recombinant adenoviruses

The present study used the mouse choline acetyltransferase (ChAT) promoter (accession number in GenBank: NC_000080), which is the regulatory element for neuronal-specific expression and includes the cholinergic-specific enhancer and a neuron-restrictive silencer element (NRSE) (Misawa et al., 1992; Lönnerberg et al., 1996). Additionally, hYARS clones that permit sub-cloning into the pAD Track-ChAT-CMV/GFP vector were used. Stable homologous recombinants of Flag-tagged pADTrack-ChAT-hYARS^{WT}-CMG/GFP, pADTrack-ChAT-hYARS^{E196K}-CMG/GFP, and pADTrack-ChAT-hYARS^{G41R}-CMG/GFP were generated using an E_1/E_3 double-deletion supercoiled adenoviral backbone vector (pADEasy-1, Stratagene; SantaClara, CA, USA). The titers used for these experiments included Ad/ChAT 6.3×10^9 (pfu/mL), AdhYARS^{WT}/ChAT 4.8×10^9 (pfu/mL), AdhYARS^{E196K}/ChAT 4.3×10^9 (pfu/mL), and AdhYARS^{G41R}/ChAT 7.1×10^9 (pfu/mL), respectively.

Viral administration

All mice were anesthetized with 30 mg/kg of Zoletil (Vibrac; CarrorsSeedees, France) and 10 mg/kg of Rompun (Bayer; Leverkusen, Germany). The sciatic nerve was exposed by an incision of the musculus gluteus superficialis, and the recombinant adenoviruses were injected into the nerve using a Hamilton syringe and glass micropipette under a stereoscope. Diluted virus solutions of AdhYARS^{WT}/ChAT (1 μL), AdhYARS^{E196K}/ChAT (1 μL), and AdhYARS^{G41R}/ChAT (1 μL) containing 0.1% fast green (tracer) were injected into the sciatic nerve of each animal, and the skin incision was closed using Silkam 4.0 sutures (B/Braun; Melsungen, Germany). The present animal model was constructed using an adenovirus injection into the sciatic nerve, but it is highly likely that the amount of injected virus varied among the administrations. Thus, each animal model may exhibit differences in the green fluorescent protein (GFP) expression patterns regardless of the type of mutant YARS.

Tissue processing

Seven days after the viral administration, the sciatic nerves, $L_{4–5}$ dorsal root ganglia (DRG), and $L_{4–5}$ spinal cord were extracted from the mice. Tissue samples were fixed overnight at 4°C using 4% paraformaldehyde (PFA) prepared in 0.1M phosphate buffer (PB) for immunohistochemistry (IHC) procedures. The samples were immersed overnight in the same solution at 4°C, transferred to 30% sucrose in 0.1 M phosphate buffer for 3 days, and then embedded in OCT compound (Leica Biosystems, Richmond, VA, USA). Dry ice was used to immediately freeze the samples before they were cryosectioned into frozen slices (16 μm) and placed onto gelatin-coated glass slides. Ice-cold phosphate-buffered saline (PBS) was used during the removal of the sciatic nerve sheaths, and the spinal cord at $L_{4–6}$ segment (dorsal and ventral horns) was cut.

Immunofluorescence labeling

For the immunofluorescence staining, the tissue sections that were placed on the gelatin-coated glass slides were fixed in 4% paraformaldehyde for 10 minutes and then washed in PBS three times. The tissues were then permeabilized in PBS containing 0.3% Triton-X 100; this was followed by blocking with 10% bovine serum albumin (BSA) at 4°C overnight. Next, the slides were incubated for 1 hour at room temperature in rabbit anti-flag (1:1,000; Cell Signaling Technology; Danvers, MA, USA), which was used as the primary antibody, followed by three washes in PBS. Subsequently, the samples were immersed in Alexa-Fluor 594 donkey anti-rabbit secondary antibody (1:1,000; Invitrogen, Life Technologies; Madison, WI, USA) for 2 hours at room temperature, washed three times in PBS, and then mounted using mounting gel. A laser scanning confocal microscope (LSM 700, Carl Zeiss; Oberkochen, Germany) was used to detect immunofluorescence on the slides.

Western blot analysis

A 10% sodium dodecyl sulfate polyacrylamide gel electrophoresis (SDS-PAGE) procedure was performed to separate the protein lysates using mouse beta-actin (1:5,000; Sigma; St. Louis, MO, USA) and rabbit anti-Flag (1:1,000; Cell Signaling Technology) primary antibodies. After the primary antibody staining, appropriate horseradish peroxide-conjugated secondary antibody staining was performed after three washes in Tris-buffered saline with Tween 20 (TBST). An enhanced chemiluminescence (ECL) procedure (Amersham; Buckinghamshire, England) was then applied, and a membrane was developed.

Statistical analysis

All data were analyzed with one-way analysis of variance (ANOVA) tests and Bonferroni posthoc tests were used for multiple comparisons. Data are expressed as the mean ± SD using SPSS 23.0 software (IBM, Armonk, NY, USA). After analyses of three independent experiments, P values < 0.001 were considered to indicate statistical significance.

Results

Different expression patterns of hYARS proteins in the spinal cord

To further characterize DI-CMTC using an *in vivo* mouse model, an adenovirus system was constructed using pAdeasy-ChAT-hYARS-Flag-CMV-GFP because this virus system is thought to express Flag-tagged hYARS under the surveillance of ChAT and GFP with the close scrutiny of a CMV (**Figure 1A**). Additionally, to determine the efficiency of in vitro hYARS protein expression in the 293 cell line, western blot analyses were performed to determine whether the constructed adenovirus exhibited normal function in terms of WT, E196K, and G41R protein expressions (**Figure 1B**). The promoter of the mouse ChAT gene, which includes a NRSE and cholinergic-specific enhancer, has previously been used in similar models because specific differences in DNA sequences linked to human diseases often have analogous sequences in the mouse genome (Cheng et al., 2014). The present study also utilized another important physiological property of the neuron, axonal transport, to retrogradely transport recombinant adenovirus-harboring mutant genes to the DRG and spinal cord (During, 2006). Finally, the constructed vectors were injected into the sciatic nerves of the mice to create WT, E196K, and G41R hYARS over-expressing mouse models. In our opinion, the use of direct injections lowers the possibility of meaningless phenotypes and allows for the administration of concentrated amounts of adenovirus for infection. Although this method may aid in the identification of clear phenotypes that are similar to hYARS-associated diseases, inexperienced handling during the injection procedure may lead to false and/or unusual results. With this limitation in mind, the present study reports the effects of two mutant genes associated with DI-CMTC in a mouse model for the first time.

Distribution defects of hYARS mutations in peripheral axons

In the spinal cord, GFP fluorescence was observed only in neuron-related peripheral projections but not in spinal glial cells because Flag was expressed only using the neuron-specific promoter. Immunolabeling was performed using an anti-Flag antibody to identify the transfected expressions of WT, E196K, and G41R YARS genes in the spinal cord. All adenovirus genes, and even the empty vector without YARS gene, exhibited GFP-positive signals in the ventral horn of the spinal cord because this expression is driven by a cytomegalovirus (CMV) promoter in the adenovirus vector (**Figure 2A**). The E196K- and WT-expressed samples exhibited anti-Flag signals in the ventral horn of the spinal cord, but the G41R mutant had relatively low signals in this region; magnified confocal images (100 μm) verified these results (**Figure 2B**). Additionally, because the empty virus vector contained only the ChAT promoter, it was unable to express YARS-Flag fusion proteins. It was quite clear that the cell bodies were positioned along a chain that was located parallel to the spinal cord inside the vertebrae, whereas the axons terminated in the spinal nerve sheaths. The presence of GFP/Flag double-positive signaling in the axons indicates that the adenoviral vector was effectively expressed in the YARS protein, which mostly occurred for the E196K mutant and WT (**Figure 2B**). These findings suggest that there were neuron-specific expressions of Flag-tagged hYARS fusion proteins in the peripheral nerves (WT and E196K); the present *in vivo* experiment did not identify any G41R expression. On the other hand, Jordanova et al. (2006) utilized *in vitro* techniques and found reductions in both the tear-drop effects and homogenous distributions of both mutant genes in most transfected cells (without preferential sorting to neuronal tips) compared with non-transfected cells.

In the present study, immunohistochemistry (IHC) procedures using an anti-Flag antibody were employed to determine the expressions of the WT, E196K, and G41R proteins in the sciatic nerve. All adenovirus vectors exhibited GFP-positive signaling due to a transcript driven by

a CMV promoter (**Figure 3A**). The number of Flag/GFP double-positive nerve fibers in the WT group was very high compared with that in the E196K mutant group (**Figures 3A** and **B**); therefore, the expression patterns of anti-Flag staining in the nerve cross-sections significantly differed between the two mutant genes (**Figure 3B**). Because anatomical differences in tissues may lead to dissimilarities in gene expression, immunofluorescence was performed with an anti-Flag antibody and revealed infected WT in the longitudinal sections of the sciatic nerve. There were relatively few Flag/GFP double-positive axons for the E196K mutation compared with the WT (**Figure 3C**); counting was based on a 300 × 300 μm^2 area (**Figure 3D**). Taken together, these findings suggest that there were possible dissimilarities in expression and differences in distribution between the WT and E196K mutant YARS groups in the present *in vivo* model. On the other hand, the G41R mutant gene was not always equally expressed in all tissues.

Distribution patterns of hYARS proteins in DRGs

Next, the expression profiles of all three adenovirus vectors in the sensory neural cell bodies of the DRG were analyzed in the infected adenovirus mouse model. Using IHC, Bellier and Kimura (2007) found that ChAT can be visualized in DRG neurons. Thus, to determine the hYARS expression levels of WT gene and the E196K and G41R mutant genes in the DRG, the expression levels of Flag-tagged hYARS were evaluated in the DRG samples 7 days after adenoviral infection. The WT gene and the E196K mutant gene both showed Flag-positive signals with GFP fluorescence (**Figure 4A**); thus, there was no difference in the protein expression levels of the WT and E196K groups, whereas the G41R mutant protein was not expressed in DRG neurons (**Figure 4B**). Taken together, these findings indicate that there were dissimilarities in the expressions of mutant genes in all expressed regions.

Discussion

For the first time, the present study utilized E196K and G41R mutations in a mouse model of DI-CMTC that has very similar features to the human disease to further characterize its etiology and pathophysiology. DI-CMTC is associated with axonal degeneration and the demyelination of peripheral motor and sensory neurons; three mutations in YARS-encoding regions have been reported (Jordanova et al., 2006). Our research group developed a DI-CMTC animal model to identify the distributions of the WT protein and the E196K and G41R mutant proteins in the spinal cord, DRG, and nerve fibers using a Flag-tagged hYARS fusion-expressing adenovirus. Because the spinal cord extends from the medulla oblongata in the brain stem to the lumbar region of the vertebral column and sensory neurons positioned in the DRG innervate the sciatic nerve via primary afferent fibers, it is relatively easy to administer an infection using an adenoviral vector (Rigaud et al., 2008). Thus, the best potential outcome from designing a mouse model would be the easy visualization of effects in a short time frame using immunostaining.

Storkebaum et al. (2009) employed an *in vivo* paradigm to investigate the cause of DI-CMTC and observed that the specific YARS expression levels of mutants in *Drosophila* neurons prompt continuous short falls in motor function that are associated with the degeneration of related axons that form a giant fiber. Moreover, the molecular pathways that are involved in this YARS-associated neurodegeneration are conserved from flies to humans. The findings obtained using this *Drosophila* model of DI-CMTC also indicate that the neuron-specific expression of mutant YARS induces impaired motor performance as well as electrophysiological and morphological neuronal defects (Storkebaum et al., 2009). Whereas the fly model generated by these authors provided mechanistic insights into the pathogenesis of DI-CMTC that defined the role of YARS in neuronal cell homeostasis, the present findings utilized a more effective adenovirus vector system that incorporated *in vivo* techniques to express YARS fusion proteins. A recent kinetic study investigating these mutations indicated that DI-CMTC is not the result of catalytic deficits in the tRNA aminoacylation reaction (Froelich and First, 2011). However, none of these studies provided experimental conclusions on Mus musculus, which suggests that the present results are novel.

A similar *in vitro* study found that CMT2D-causing mutations associated with GARS share the same defects in terms of localization (Nangle et al., 2007). Furthermore, previous findings from our research group have detailed the roles of GARS and mutant genes that are associated with distributional defects in WT genes in CMT2D using a mouse model (Seo et al., 2014b). Jordanova et al. (2006) utilized the Y24815 strain of *Sachromyces cerevisiae* (*in vivo*) and observed a partial loss of aminoacylation activity in the mutant protein as well as reductions in yeast growth based on genetic complementation and biochemical experiments. Additionally, the *in vitro* results from that study showed a reduced and homogenous distribution of the mutant protein in transfected cells compared with differences in localization between neuronal and non-neuronal cells as well as differences in the numbers of differentiating and undifferentiated neuronal cells in non-transfected cells. These authors concluded that the mutations abridged the initial step of the aminoacylation reaction and that there was a dominant negative effect on WT function, including deficits in synaptic plasticity that likely led to the ultimate motor and sensory peripheral neuropathies (Jordanova et al., 2006). Thus, in an attempt to identify a similar type of distributional difference using an *in vivo* model of DI-CMTC, YARS mutants were injected into mice, and a defect in YARS mutant localization was confirmed.

The ventral horn of the spinal cord encompasses motor neurons and their axons, which extend through the cell bodies to peripheral nerves to directly influence the activity of axial muscles. Following the transfection of the YARS WT-, E196K-, and G41R-expressing virus vectors into the sciatic nerve, there were equal expressions of the YARS WT and E196K fusion proteins according to the Flag-tagged expressions in each portion of the spinal cord. On the other hand, expression of the G41R fusion proteins was not evident in the ventral horn. These findings clearly indicate that mea-

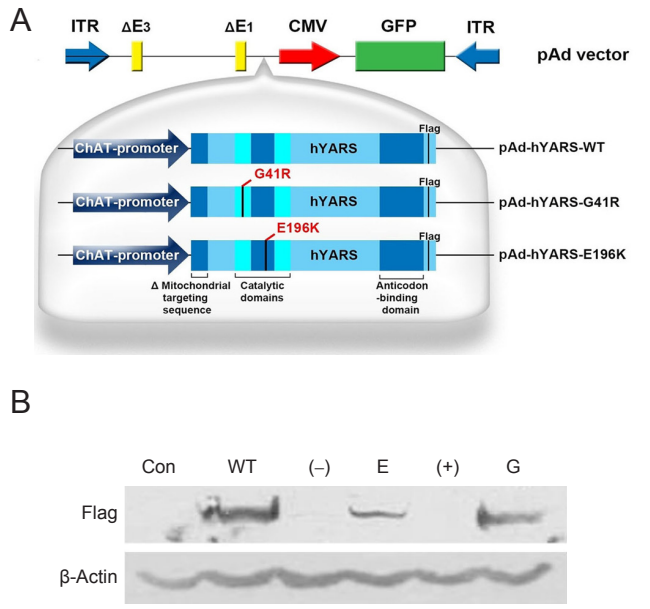

Figure 1 Genomic structures of the human tyrosyl-tRNA synthetase (hYARS)-expressing adenoviral vectors and their expression patterns in the cell line.
(A) Schematic representations of the expression units and promoter of each constructed adenovirus (YARS WT, E196K, and G41R). The mitochondrial targeting sequence was deleted to prevent the YARS proteins from being expressed in mitochondria; because mitochondria have their own protein synthesis system, the expression of the mutated YARS in mitochondria may affect the distribution pattern of the adenovirus in the cytoplasm of long-distance peripheral nerves. To avoid this possibility, the mitochondrial targeting sequence was deleted to reduce the chances of adenovirus expression in mitochondria. (B) Protein lysates from adenovirus-infected mouse sciatic nerves analyzed with western blots. Con: No virus; WT: wild-type; (–): empty virus without ChAT; E: E196K mutant hYARS; (+): empty virus with ChAT; G: G41R mutant hYARS. Flag-YARS: 59 kDa; β-actin: 42 kDa. All experiments were performed in triplicate.

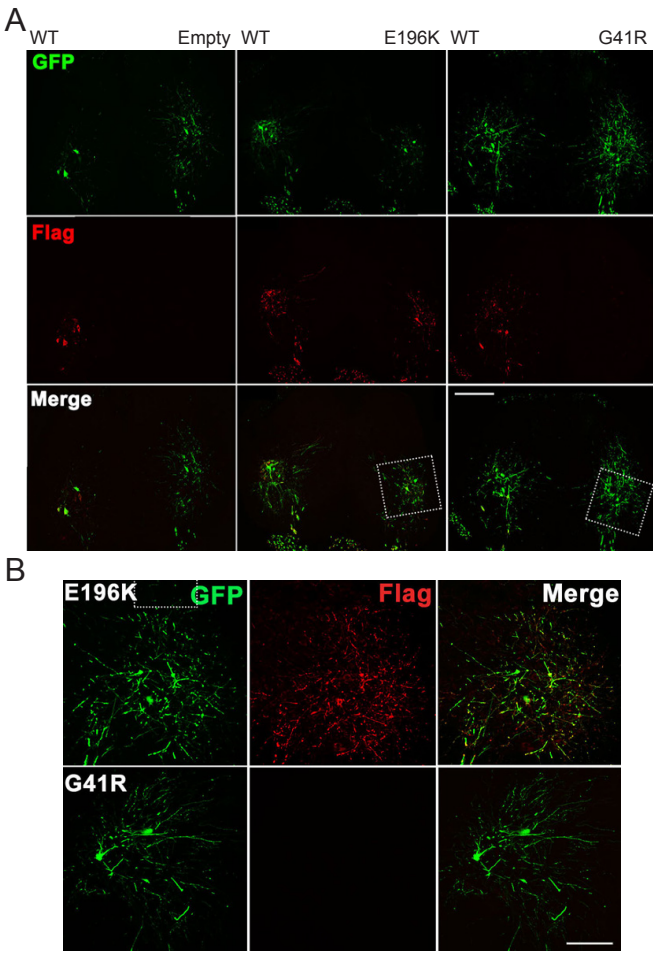

Figure 2 Distribution pattern of human tyrosyl-tRNA synthetase (hYARS) in the spinal cord.
(A) Neuron-specific expression of wild type (WT) YARS (hYARS) in spinal cord sections using green fluorescent protein (GFP) expression (green) and the immunofluorescence labeling of Flag (red); yellow staining indicates the overlapping of red and green signals. GFP/Flag double-positive signals indicate the expression of Flag-tagged hYARS fusion proteins in the spinal cord. Empty: Empty virus without insert; WT: wild-type; E196K: E196K mutant hYARS; G41R, G41R mutant hYARS. Scale bar: 500 μm. (B) Magnified visualization of the E196K and G41R mutant hYARS expressions in the spinal cord. Scale bar: 100 μm. Three independent experiments were performed for each immunohistochemistry analysis.

surements of the expressions of mutant YARS proteins administered with an adenovirus vector are able to characterize the molecular, morphological, and functional phenotypes of DI-CMTC in this animal model. Additionally, the present experimental data provide clear evidence that there are differences in the distribution of the mutant genes or dissimilarities in the expression of the proteins in the mutant genes in the same expressed regions; moreover, the phenotype of the animal model developed sufficiently in just 7 days and revealed the distribution of the mutant proteins.

There were fewer $Flag^+/GFP^+$ axons in the longitudinal sections of the sciatic nerve with the mutant YARS relative to in the WT group, which is also strong evidence of distributional differences in peripheral axons in this *in vivo* model. These distributional defects may depend on axon length and may be the result of impaired axonal transport due to the altered non-canonical effects of the mutant YARS (Hurd and Saxton, 1996). According to this hypothesis, the lack of YARS in peripheral axons distal from the motor neuron cell body may affect the synthesis of axonal transport-associated proteins and ultimately induce axonal degradation. Neurons require the efficient axonal transportation of cytoskeletal vesicle components, mitochondria, and synaptic vesicles, and avariety of genes associated with CMT are related to axonal transport in the PNS (Jordanova et al., 2006). Thus, long and narrow peripheral axons that are subjected to length-dependent distributional defects may result in a neuronal specificity for the YARS mutation. Length-dependent axonal degradation is a major etiological factor associated with inherited peripheral neuropathies that begin in the distal part of a nerve and spread toward the cell body (Seo et al., 2014a). This may also explain why there is a reduced expression of the G41R mutant, whereas other factors may cause the anatomical differences in the expressed regions and the entire *in vivo* system. This distribution defect may also have a negative effect on the axon terminals of long-distance peripheral nerves; therefore, additional studies are needed to

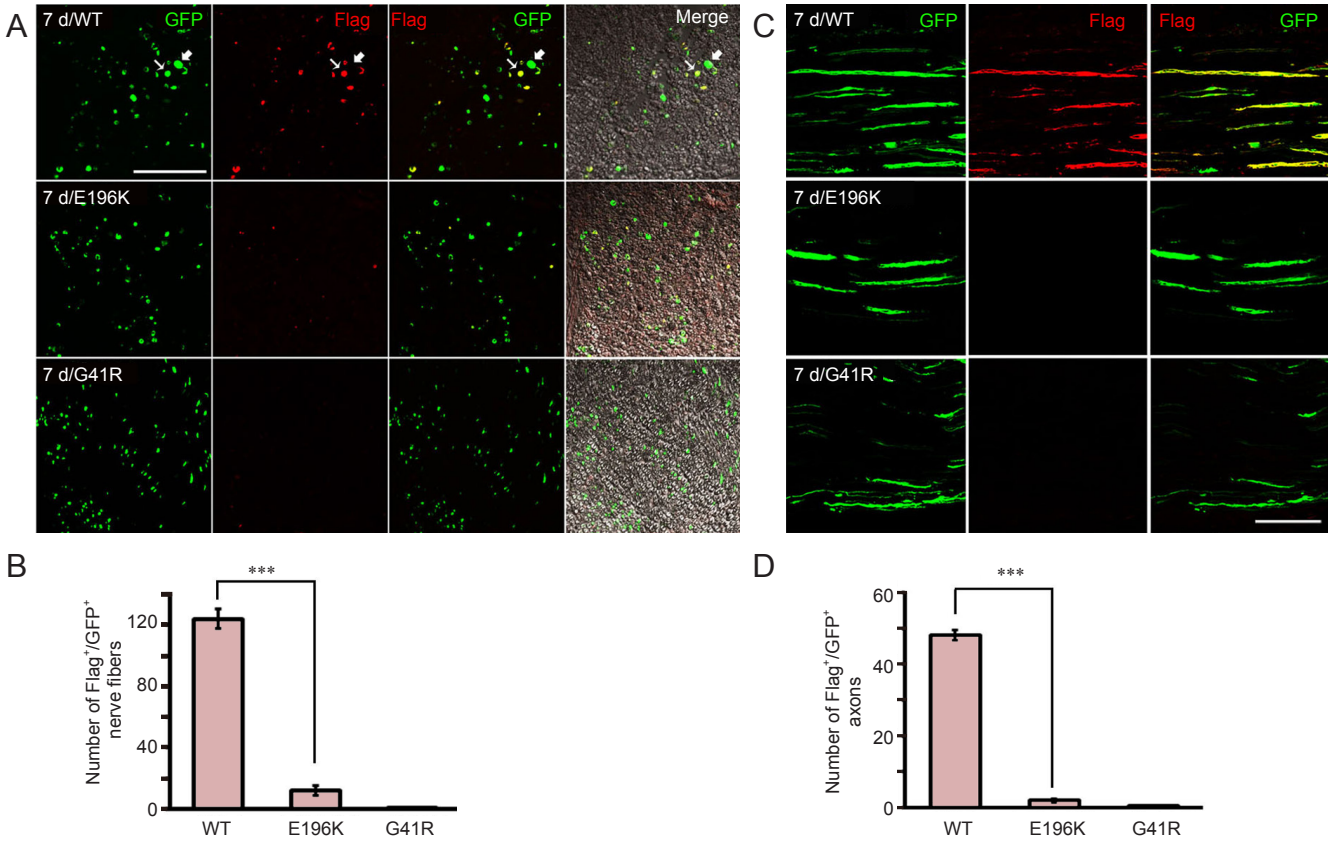

Figure 3 Neuron-specific expressions of human tyrosyl-tRNA synthetase (hYARS) in the sciatic nerves.
(A) Neuron-specific expressions of hYARS proteins in cross-sections of sciatic nerves using green fluorescent protein (GFP) expression (green) and the immunofluorescence labeling of Flag (red); yellow staining indicates the overlapping of red and green signals with Flag-tagged hYARS fusion proteins (GFP/Flag double-staining, narrow arrow). Bold arrows depict GFP-expressing nerve fibers without Flag expression. Scale bar: 40 μm. (B) Quantification of $Flag^+/GFP^+$ nerve fibers showed the number of axons with Flag immunoreactivity out of GFP^+ nerve fibers in a 300 × 300 μm^2 area; ***$P < 0.0001$, *vs.* wild type (WT) YARS ($n = 5$). Three independent experiments were performed for each immunohistochemistry analysis. (C) Immunofluorescence procedure with an anti-Flag antibody in the infected WT gene and E196K and G41R mutants in a longitudinal section of the sciatic nerve; yellow staining indicates the overlapping of green and red signals with Flag-tagged hYARS fusion protein. Scale bar: 50 μm. (D) Numbers of $Flag^+/GFP^+$ axons in WT and mutants; counting the number of axons with Flag immunoreactivity out of GFP^+ nerve fibers was performed in a 300 × 300 μm^2 area (***$P < 0.0001$; $n = 5$). Three independent experiments were performed for each immunohistochemistry analysis.

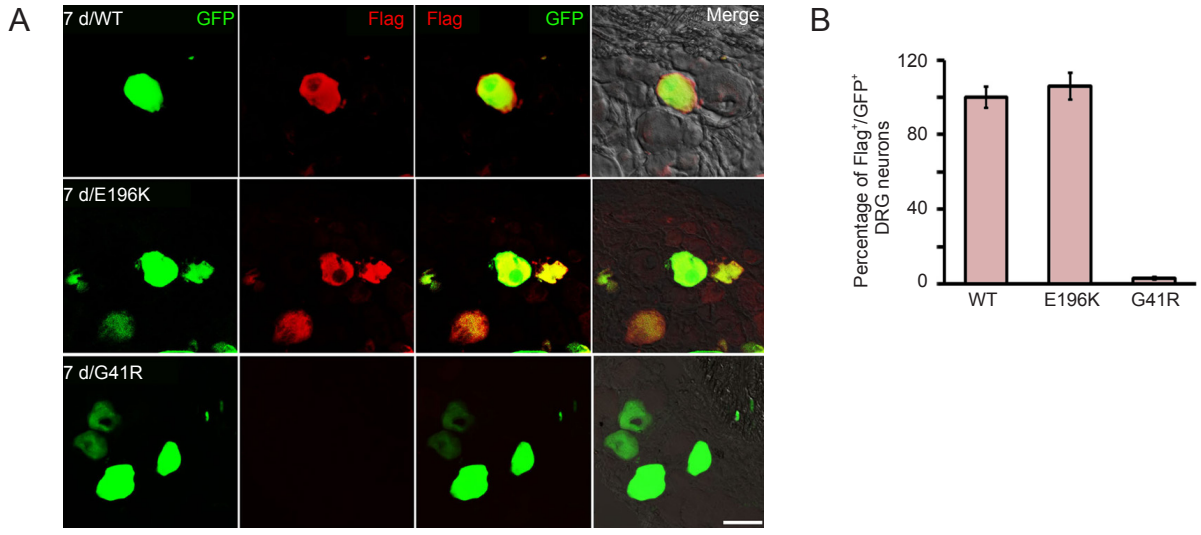

Figure 4 Expression patterns of human tyrosyl-tRNA synthetase (hYARS) in dorsal root ganglia (DRG) neuronal cell bodies.
(A) Expression of Flag-tagged hYARS fusion proteins in DRG neuronal cell bodies. Immunofluorescence analyses of the Flag (red) and GFP (green) expressions in the DRG are shown. Scale bar: 40 μm. (B) Percentages of $Flag^+/GFP^+$ DRG neurons for all adenoviruses; quantitative analyses show the number of DRGs with Flag immunoreactivity out of GFP^+ DRGs in a 300 × 300 μm^2 area. Three independent experiments were performed for each immunohistochemistry analysis.

identify the cause of distributional defects of mutant YARS proteins to aid in an understanding the pathophysiology underlying this incurable disease.

Nangle et al. (2007) found similar distributional defects in all studied CMT-associated mutant GARS proteins, whereas Jordanova et al. (2006) identified different subcellular distributions of YARS in neuronal and non-neuronal cells, which they referred to as the tear-drop effect. In other words, this axonal degeneration is due to the exclusion of mutant YARS proteins in anterograde and retrograde cargo transport and the inability of axons to clear the mutant proteins (Motley et al., 2010). Studies investigating dimer interactions and formations in subjects with these disease-related mutations may provide strong data regarding the manifestation of these distributional defects.

Although a variety of novel approaches have been developed to treat CMT, this disease remains incurable. The clinical and genetic heterogeneity of DI-CMTC as well as the large number of genes linked to this disease pose a challenge to the identification of therapeutic strategies and, thus, animal models of DI-CMTC can be powerful tools. The development of animal models and the reproduction of phenotypes comparable to DI-CMTC will aid in the design of new therapeutic approaches, modifiers, biomarkers, and molecular mechanisms that can lead to clinical trials. Although DI-CMTC exhibits clear phenotypes in both peripheral axons and Schwann cells, the primary focus of our research group remains the distributional defects of mutated YARS in axons. However, further studies evaluating Schwann cells as a factor underlying the pathophysiology of DI-CMTC should be conducted using Schwann cell-specific adenovirus vectors.

Acknowledgments: *We thank Muwoong Kim, Nicholas Asiimwe and Ulfuara Shefa (Department of Anatomy and Neurobiology, Kyung Hee University, Seoul, Korea) for valuable discussion.*

Author contributions: *JJ and YH conceived and designed the study. SL and HWJ carried out the experiments. SL, SP, JC, MSK, NYJ, IOS, JJ and YH analyzed the data. SP, JJ and YH wrote the paper. All authors approved the final version of this paper*

Conflicts of interest: *None declared.*

Plagiarism check: *This paper was screened twice using CrossCheck to verify originality before publication.*

Peer review: *This paper was double-blinded and stringently reviewed by international expert reviewers.*

References

Antonellis A, Green ED (2008) The role of aminoacyl-tRNA synthetases in genetic diseases. Annu Rev Genomics Hum Genet 9:87-107.

Bellier JP, Kimura H (2007) Acetylcholine synthesis by choline acetyltransferase of a peripheral type as demonstrated in adult rat dorsal root ganglion. J Neurochem 101:1607-1618.

Charcot JM, Marie P (1886) Sur une forme particuliore d'atrophie musculaire progressive, souvent familiale d6butant par les pieds et les jambes et atteignant plus tards les mains. Rev Med 6:97-138.

Cheng Y, Ma Z, Kim BH, Wu W, Cayting P, Boyle AP, Sundaram V, Xing X, Dogan N, Li J (2014) Principles of regulatory information conservation between mouse and human. Nature 515:371-375.

Davis CJ, Bradley WG, Madrid R (1978) The peroneal muscular atrophy syndrome: clinical, genetic, electrophysiological and nerve biopsy studies. I. Clinical, genetic and electrophysiological findings and classification. J Genet Hum 26:311-349.

During MJ (2006) Gene therapy of the central nervous system: from bench to bedside. Gulf Professional Publishing.

Fersht AR, Ashford JS, Bruton CJ, Jakes R, Koch GL, Hartley BS (1975) Active site titration and aminoacyl adenylate binding stoichiometry of aminoacyl-tRNA synthetases. Biochemistry 14:1-4.

Froelich CA, First EA (2011) Dominant Intermediate Charcot-Marie-Tooth disorder is not due to a catalytic defect in tyrosyl-tRNA synthetase. Biochemistry 50:7132-7145.

Hoffmann J (1889) Ueber progressive neurotische Muskelatrophie. Arch Psychiatr Nervenkr 20:660-713.

Hurd DD, Saxton WM (1996) Kinesin mutations cause motor neuron disease phenotypes by disrupting fast axonal transport in Drosophila. Genetics 144:1075-1085.

Jordanova A, Irobi J, Thomas FP, Van Dijck P, Meerschaert K, Dewil M, Dierick I, Jacobs A, De Vriendt E, Guergueltcheva V, Rao CV, Tournev I, Gondim FA, D'Hooghe M, Van Gerwen V, Callaerts P, Van Den Bosch L, Timmermans JP, Robberecht W, Gettemans J, et al. (2006) Disrupted function and axonal distribution of mutant tyrosyl-tRNA synthetase in dominant intermediate Charcot-Marie-Tooth neuropathy. Nat Genet 38:197-202.

Kennerson ML, Zhu D, Gardner RJ, Storey E, Merory J, Robertson SP, Nicholson GA (2001) Dominant intermediate Charcot-Marie-Tooth neuropathy maps to chromosome 19p12-p13. 2. Am J Hum Genet 69:883-888.

Kleeman TA, Wei D, Simpson KL, First EA (1997) Human tyrosyl-tRNA synthetase shares amino acid sequence homology with a putative cytokine. J Biol Chem 272:14420-14425.

Krajewski KM, Lewis RA, Fuerst DR, Turansky C, Hinderer SR, Garbern J, Kamholz J, Shy ME (2000) Neurological dysfunction and axonal degeneration in Charcot-Marie-Tooth disease type 1A. Brain 123:1516-1527.

Lönnerberg P, Schoenherr CJ, Anderson DJ, Ibáñez CF (1996) Cell type-specific regulation of choline acetyltransferase gene expression role of the neuron-restrictive silencer element and cholinergic-specific enhancer sequences. J Biol Chem 271:33358-33365.

Misawa H, Ishii K, Deguchi T (1992) Gene expression of mouse choline acetyltransferase. Alternative splicing and identification of a highly active promoter region. J Biol Chem 267:20392-20399.

Motley WW, Talbot K, Fischbeck KH (2010) GARS axonopathy: not every neuron's cup of tRNA. Trends Neurosci 33:59-66.

Nangle LA, Zhang W, Xie W, Yang XL, Schimmel P (2007) Charcot–Marie–Tooth disease-associated mutant tRNA synthetases linked to altered dimer interface and neurite distribution defect. Proc Natl Acad Sci 104:11239-11244.

Pruitt KD, Tatusova T, Klimke W, Maglott DR (2009) NCBI Reference Sequences: current status, policy and new initiatives. Nucleic Acids Res 37:D32-36.

Rigaud M, Gemes G, Barabas ME, Chernoff DI, Abram SE, Stucky CL, Hogan QH (2008) Species and strain differences in rodent sciatic nerve anatomy: implications for studies of neuropathic pain. Pain 136:188-201.

Seo AJ, Park BS, Jung J (2014a) GRS defective axonal distribution as a potential contributor to distal spinal muscular atrophy type V pathogenesis in a new model of GRS-associated neuropathy. J Chem Neuroanat 61-62:132-139.

Seo AJ, Shin YH, Lee SJ, Kim D, Park BS, Kim S, Choi KH, Jeong NY, Park C, Jang JY, Huh Y, Jung J (2014b) A novel adenoviral vector-mediated mouse model of Charcot-Marie-Tooth type 2D (CMT2D). J Mol Histol 45:121-128.

Storkebaum E, Leitão-Gonçalves R, Godenschwege T, Nangle L, Mejia M, Bosmans I, Ooms T, Jacobs A, Van Dijck P, Yang XL, Schimmel P, Norga K, Timmerman V, Callaerts P, Jordanova A (2009) Dominant mutations in the tyrosyl-tRNA synthetase gene recapitulate in Drosophila features of human Charcot–Marie–Tooth neuropathy. Proc Natl Acad Sci U S A 106:11782-11787.

Tooth HH (1886) The peroneal type of progressive muscular atrophy. H. K. Lewis, London.

Copyedited by Li CH, Song LP, Zhao M